Phonon induced line broadening and population of the dark exciton in a deeply trapped localized emitter in monolayer WSe_2

Yu-Ming He,[1] Sven Höfling[1,2] and Christian Schneider[1,*]

[1] *Technische Physik and Wilhelm Conrad Röntgen Research Center for Complex Material Systems, Physikalisches Institut, Universität Würzburg, Am Hubland, D-97074 Würzburg, Germany*

[2] *SUPA, School of Physics and Astronomy, University of St Andrews, St Andrews, KY16 9SS, United Kingdom*

[*] *christian.schneider@physik.uni-wuerzburg.de*

Abstract: We study trapped single excitons in a monolayer semiconductor with respect to their temperature stability, spectral diffusion and decay dynamics. In a mechanically exfoliated WSe_2 sheet, we could identify discrete emission features with emission energies down to 1.516 eV which are spectrally isolated in a free spectral range up to 80 meV. The strong spectral isolation of our localized emitter allow us to identify strong signatures of phonon induced spectral broadening for elevated temperatures accompanied by temperature induced luminescence quenching. A direct correlation between the droop in intensity at higher temperatures with the phonon induced population of dark states in WSe_2 is established. While our experiment suggests that the applicability of monolayered quantum emitters as coherent single photon sources at elevated temperatures may be limited, the capability to operate them below the GaAs band-edge makes them highly interesting for GaAs-monolayer hybrid quantum photonic structures.

OCIS codes: ¨(310.0310) Thin films;¨

References and links

[1] P. Michler, A. Kiraz, C. Becher, W. V. Schoenfeld, P. M. Petroff, L. Zhang, E. Hu, and A. Imamoglu, "A quantum dot single-photon turnstile device," Science **290**, 2282–2285 (2000).

[2] F. Diedrich and H. Walther, "Nonclassical radiation of a single stored ion," Phys. Rev. Lett. **58**, 203–206 (1987).

[3] K. De Greve, S. Clark, D. Sleiter, K. Sanaka, T. Ladd, M. Panfilova, A. Pawlis, K. Lischka, and Y. Yamamoto, "Photon antibunching and magnetospectroscopy of a single fluorine donor in ZnSe," Applied Physics Letters **97**, 241913 (2010).

[4] F. Fuchs, B. Stender, M. Trupke, D. Simin, J. Pflaum, V. Dyakonov, and G. Astakhov, "Engineering near-infrared single-photon emitters with optically active spins in ultrapure silicon carbide," Nature communications **6**, 7578 (2015).

[5] Y.-M. He, G. Clark, J. R. Schaibley, Y. He, M.-C. Chen, Y.-J. Wei, X. Ding, Q. Zhang, W. Yao, X. Xu, C.-Y. Lu, and J.-W. Pan, "Single quantum emitters in monolayer semiconductors," Nature nanotechnology **10**, 497–502 (2015).

[6] M. Koperski, K. Nogajewski, A. Arora, V. Cherkez, P. Mallet, J.-Y. Veuillen, J. Marcus, P. Kossacki, and M. Potemski, "Single photon emitters in exfoliated WSe_2 structures," Nature nanotechnology **10**, 503–506 (2015).

[7] C. Chakraborty, L. Kinnischtzke, K. M. Goodfellow, R. Beams, and A. N. Vamivakas, "Voltage-controlled quantum light from an atomically thin semiconductor," Nature nanotechnology **10**, 507–511 (2015).

[8] A. Srivastava, M. Sidler, A. V. Allain, D. S. Lembke, A. Kis, and A. Imamoğlu, "Optically active quantum dots in monolayer WSe_2," Nature nanotechnology **10**, 491–496 (2015).

[9] P. Tonndorf, R. Schmidt, R. Schneider, J. Kern, M. Buscema, G. A. Steele, A. Castellanos-Gomez, H. S. J. van der Zant, S. M. de Vasconcellos, and R. Bratschitsch, "Single-photon emission from localized excitons in an atomically thin semiconductor," Optica **2**, 347–352 (2015).

[10] X. Xu, W. Yao, D. Xiao and T. F. Heinz, "Spin and pseudospins in layered transition metal dichalcogenides," Nature Phys **10**, 343–350 (2014).

[11] A. M. Jones, H. Yu, N. J. Ghimire, S. Wu, G. Aivazian, J. S. Ross, B. Zhao, J. Yan, D. G. Mandrus, D. Xiao, W. Yao and X. Xu, "Optical generation of excitonic valley coherence in monolayer WSe_2," Nature nanotechnology **8**, 634–638 (2013).

[12] D. Xiao, G. B. Liu, W. Feng, X. Xu, and W. Yao, "Coupled spin and valley physics in monolayers of MoS_2 and other Group-VI dichalcogenides." Phys Rev Lett **108**, 196802 (2012).

[13] K. F. Mak, K. He, J. Shan and T. F. Heinz, "Control of valley polarization in monolayer MoS_2 by optical helicity." Nature nanotechnology **7**, 494–498 (2012).

[14] T. Cao, G. Wang, W. Han, H. Ye, C. Zhu, J. Shi, Q. Niu, P. Tan, E. Wang, B. Liu and J. Feng, "Valley-selective circular dichroism of monolayer molybdenum disulphide." Nature communications **3**, 887 (2012).

[15] H. Zeng, J. Dai, W. Yao, D. Xiao and X. Cui, "Valley polarization in MoS_2 monolayers by optical pumping." Nature nanotechnology **7**, 490–493 (2012).

[16] Y. J. Zhang, T. Oka, R. Suzuki, J. T. Ye and Y. Iwasa, "Electrically switchable chiral light-emitting transistor." Science **344**, 725–728 (2014).

[17] K. F. Mak, K. L. McGill, J. Park and P. L. McEuen, "The valley Hall effect in MoS_2 transistors." Science **344**, 1489–1492 (2014).

[18] E. J. Sie, J. W. Mclver, Y. H. Lee, L. Fu, J. Kong and N. Gedik, "Valley-selective optical Stark effect in monolayer WS_2." Nature Mater. **14**, 290–294 (2015).

[19] J. Kim, X. Hong, C. Jin, S. Shi, C. Chang, M. Chiu, L. Li and F. Wang, "Ultrafast generation of pseudo-magnetic field for valley excitons in WSe_2 monolayers." Science **346**, 1205–1208 (2014).

[20] S. Kumar, A. Kaczmarczyk, and B. D. Gerardot, "Strain-induced spatial and spectral isolation of quantum emitters in mono-and bi-layer WSe_2," Nano letters **15**, 7567–7573(2015).

[21] J. Seufert, R. Weigand, G. Bacher, T. Kümmell, A. Forchel, K. Leonardi, and D. Hommel, "Spectral diffusion of the exciton transition in a single self-organized quantum dot," Applied Physics Letters **76**, 1872–1874 (2000).

[22] M. Bayer and A. Forchel, "Temperature dependence of the exciton homogeneous linewidth in $In_{0.60}Ga_{0.40}$As/GaAs self-assembled quantum dots," Physical Review B **65**, 041308 (2002).

[23] O. Labeau, P. Tamarat, and B. Lounis, "Temperature dependence of the luminescence lifetime of single CdSe/ZnS quantum dots," Physical Review Letters **90**, 257404 (2003).

[24] B. Pietka, J. Suffczynski, M. Goryca, T. Kazimierczuk, A. Golnik, P. Kossacki, A. Wysmolek, J. A. Gaj, R. Stepniewski, and M. Potemski, "Photon correlation studies of charge variation in a single GaAlAs quantum dot," Physical Review B **87**, 035310 (2013)

[25] K. S. Novoselov, D. Jiang, F. Schedin, T. J. Booth, V. V. Khotkevich, S. V. Morozov, and A. K. Geim, "Two-dimensional atomic crystals," Proc. Natl Acad. Sci. USA **102**, 10451–10453 (2005)

[26] X. X. Zhang, Y. You, S. Y. F. Zhao, and T. F. Heinz, "Experimental Evidence for Dark Excitons in Monolayer WSe_2," Phys Rev Lett **115**, 257403 (2015)

1. Introduction

Solid state quantum emitters, such as semiconductor quantum dots [1], NV centers in diamond [2] optically active defects in semiconductors [3] or insulators [4] are promising candidates as quantum light sources or systems to host stationary quantum bits. Monolayer semiconductors have emerged as a new material platform in photonics which promises new scientific advances and technological applications: They represent a unique system to investigate robust excitonic effects due to strongly enhanced carrier binding energies, and give rise to a new class of spinor effects related to the valley pseudospin [10]. Strong progress has been made in studying such effects, including the observation of the valley pseudospin and valley polarization control[11–15]. Recently, localized excitons hosted in monolayered semiconductors have been identified as a new class of solid state quantum emitters [5–9]. Thus far, except one recent report [20], the emission wavelength of these emitters was mainly found in the spectral range between 730 and 770 nm (1.6-1.7 eV) and evolved from a rather dense emitter array. This makes it challenging to spectrally isolate single emitter lines, and imposes major obstacles to combine them with well-established GaAs based photonic devices and microcavity architectures due to the spectral absorbtion in GaAs. The photonic engineering of these structures, however, is an almost stringent prerequisite to make these emitters competitive in the zoo of quantum light sources, since thus far, signal to noise ratios remained comparably modest in these new kind of non-classical light source. In this paper, we report on the investigation of deeply localized quantum emitters hosted in a single sheet layer of WSe_2, which emit in the transparency region of undoped GaAs. The quantum emitters are red-shifted up to 180 meV with respect to the free exciton band in WSe_2, emit in a free spectral range up to 80 meV and thus can be combined

with GaAs based photonic devices in the future. We map out the temperature dependence of single localized exciton luminescence, including the thermal activation of carriers leading to temperature induced luminescence quenching, phonon induced line broadening and study recombination lifetimes of these localized defects. The temperature dependence of the single localized emitter provides the new insight of the basic level structure and exciton recombination mechanisms.

2. Experimental details

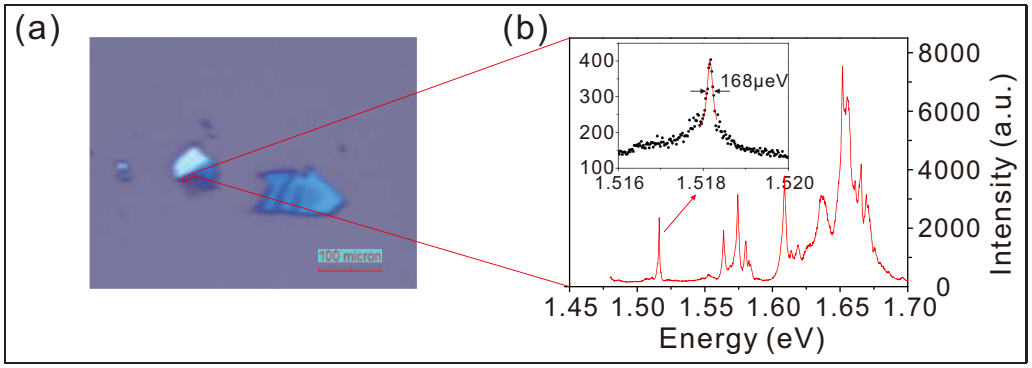

Fig. 1. (a) Optical image of an exfoliated flake on top of the Si/SiO_2 substrate. (b) Photoluminescence spectrum from localized emitters. The inset is a high resolution spectrum of the highly redshift peak (SQE_A). The data was recorded at a nominal temperature of 4.2 K.

Fig. 1(a) shows the optical image of the sample under consideration for the present study. The size of the monolayer region on the flake size is around 30μm*50μm. The flakes were obtained by mechanical exfoliation from bulk WSe_2 crystal onto a Si substrate with a 285nm SiO_2 layer on top. We followed a procedure as recently described in [25]. We used commercial 19mm tape (Scotch) to transfer the flake onto a target substrate. The substrates were cleaned with oxygen plasma before the exfoliation. Monolayer candidates of WSe_2 were pre-selected from the white light image contrast on the CCD in our optical microscope. The large light blue transparent area near the rectangle marker in Fig. 1(a) was expected to be the monolayer area, which was confirmed by low temperature non-resonant micro-photoluminescence (μPL) via the characteristic luminescence from the free exciton. For the optical experiments, the sample was attached to the cold-finger of a liquid Helium flow cryostat and the luminescence from the flake was collected by a 50x objective (NA=0.42) in a confocal microscope system. The WSe_2 flake was excited by a Continuous-Wave(CW) 532 nm laser, or a mode locked, up-converted Ti:Sa oscillator with a pulse frequency of 82 MHz and a pulse length of 3 ps. Photoluminescence measurement were performed using a Princeton-Instrument SP2750i spectrometer equipped with a liquid nitrogen cooled charge coupled detector. Fig. 1(b) shows an exemplary spectrum of the photoluminescence stemming from the interface region between the monolayer and the WSe_2 bulk region, recorded at an excitation power of 30 μW and a nominal sample temperature of 4.2 K. The spectrum is dominated by a zoo of sharp spectral lines near the rectangle area in Fig. 1(a), that are red shifted by 40-180 meV from the WSe_2 free valley exciton. In the energy range from 1.5 1.6 eV, we found dominant emission features at energies down to 1.517 eV, which are spectrally isolated by more than 80 meV from any other pronounced spectral resonance in the monolayer crystal. The inset of Fig. 1(b) shows a close-up spectrum of this spectral feature around 1.517eV (labeled as SQE_Ain the following), which is red-shifted 180meV from the 2D

exciton (1.7eV). The Lorentzian fit (red line) yields a rather narrow linewidth of 168 μeV, which is roughly two orders of magnitude smaller than the luminescence linewidth of the free exciton, and compares well with previously reported linewidth from localized excitons in WSe_2 [5–9] .

3. Results and discussion

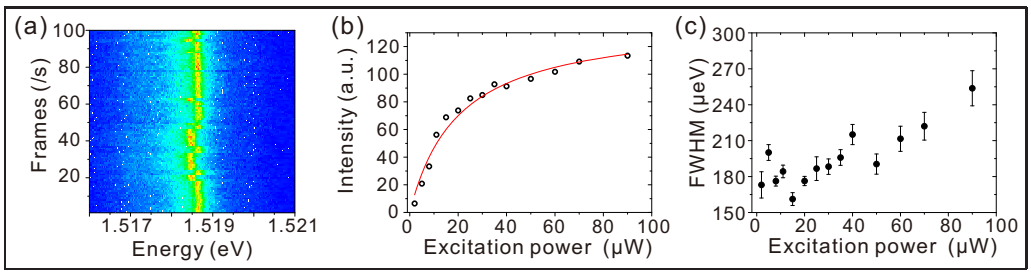

Fig. 2. (a) Spectral wandering of the SQE_A as a function of photon energy and frames. (b) The integrated counts of the photon emission from SQE_A showing the onset of a characteristic saturation behavior with increasing laser power. The red line is the saturation curve fit. (c) Linewidth of the SQE_A as a function of the excitation power.

In order to assess the influence of spectral wandering on the macroscopic time scale on the emission properties of this spectral emitter on the surface of our sample, we record various spectra every second and plotted it in the contour graph in Fig. 2(a). Clear fluctuation effects and spectral jumps occur on a timescale of seconds, a clear feature of spectral diffusion in quantum emitters [21, 24]. Such behavior is commonly observed in surface sensitive defect luminescence and has been previously identified for WSe_2 single defect luminescence in the spectral range around 750 nm [5]. Indeed, the strong interaction of the emitters close to the surface with their environment can be considered as an appealing resource for exciton-based sensing applications. Next, we investigate the power dependent emission characteristics from this emitter. In Fig. 2(b) we plot the integrated emission intensity as a function of excitation power P. We observe a clear deviation from a linear behaviour, as expected for for a two level fermionic system: The red line in Fig. 2(b) is a saturation curve fitted with the formula:

$$I(P) = I_{max}\frac{1}{1+\frac{P_0}{P}} \tag{1}$$

Here, the P_0 is the saturation power which is related to the lifetime of the excited emitter state, which corresponds to the laser power P_0=20 μW on the objective. For increasing excitation power, we furthermore observe the common power broadening effects inherent to single emitters in the presence of dephasing, as can be seen in Fig. 2(c).

The sample temperature has a strong influence on the energy and linewidth of the single localized emitter on the flake: In Fig. 3(a) and Fig. 3(c) we plot spectra from two single quantum emitters SQE_A (at 1.517eV) and SQE_B (emitting at 1.576eV) for various sample temperatures. By increasing the sample temperature, both peaks are subject to a distinct redshift, caused by the shrinking of the bandgap of the host material. To determine the broadening of the single quantum emitters, Fig. 3(b) and Fig. 3(d) depict the temperature dependent linewidth of SQE_A and SQE_B. We can reproduce these data by accounting for contributions of acoustic and optical phonon scattering in a similar manner as in conventional semiconductor QDs [22] via

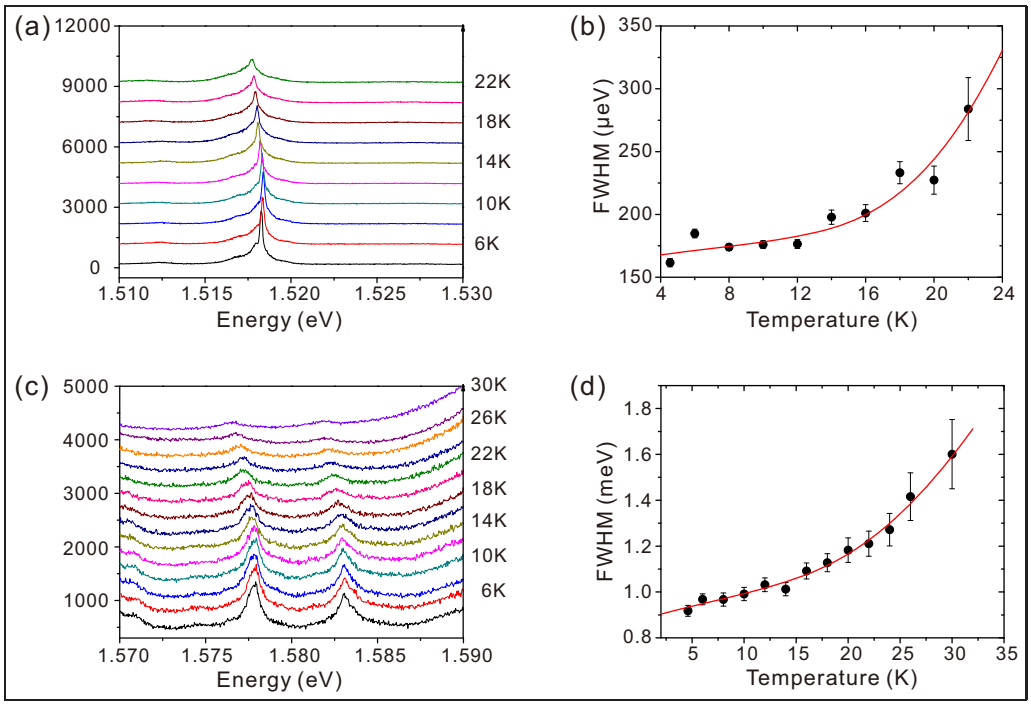

Fig. 3. (a) and (c) Temperature-dependent photoluminescence spectra of SQE$_A$ and SQE$_B$. The linewidths broaden when the temperature is increased. (b) and (d) Extracted linewidth as a function of the temperature. The red lines are fitted by equation (2).

$$\gamma(T) = \gamma_0 + \gamma_{ac} * T + \frac{\gamma_{LO}}{e^{\frac{E_{LO}}{kT}} - 1} \tag{2}$$

Where γ_0 is the linewidth at T=0, γ_{ac} and γ_{LO} give the acoustic and optical phonon scattering and E_{LO} is the activation energy of longitudinal optical phonons. In the low temperature regime the linear term, which indicates a line broadening via coupling to acoustic phonons dominates and the fit reveals $\gamma_{ac,A}$=(1.6±0.7) μeV/K and $\gamma_{ac,B}$=(11±1.0) μeV/K. At higher temperature, the linewidth dependence is dominated by the influence of the optical phonons. For both peaks, the extracted activation energy of the optical phonons yields E_{LO}=(9.94±0.60) meV and (9.28±0.48) meV for SQE$_A$ and SQE$_B$ respectively. From the intersect with the y-axis, we find the extrapolated single peak linewidth at 0 K of $\gamma_{0,A}$=(0.16±0.01) meV and $\gamma_{0,B}$=(0.88±0.02) meV which implies that the effects of spectral diffusion act significantly stronger on the high energy exciton in our case.

In addition to the temperature induced line broadening, we observe a pronounced intensity droop of the single emitter line at elevated temperatures. Figs 4(a) and Figs 4(b) depict the integrated counts as a function of T for SQE$_A$ and SQE$_B$. The data can be reproduced by a simple model, taking into account competing loss channels which can be activated by a characteristic energy (E_1 and E_2 in the case of two channels), respectively. This rate equation model yields the analytical formula:

$$I(T) = \frac{I_0}{1 + A_1 e^{\frac{E_1}{kT}} + A_2 e^{\frac{E_2}{kT}}} \tag{3}$$

Where I_0 is the extracted integrated single emitter intensity at 0K and A_1, A_2 describe the proportion of both loss channels. The activation energies E_1 and E_2 are corresponding to the two different loss channels. For SQE$_A$, we reproduced the experimental data by taking into account only one significant loss channel with a characteristic energy E_A=(9.05± 0.97)meV. For SQE$_B$, which is somewhat more blue-shifted, we yield E_{1B}=(4.25±0.44) meV, E_{2B}=(15.64±0.80) meV as characteristic energies, where the contribution of the larger energy scale is dominating the overall behavior. As the activation energy of a localized exciton into a continuum state amounts to hundreds of meV and higher shells of the confined exciton modes were identified to be several tens of meV apart [9], we assume that a thermally activated carrier transfer in a near lying dark exciton state can be the reason for the intensity quenching at elevated temperatures. This assumption is supported by the fact, that the characteristic activation energy E_A almost perfectly coincides with the identified phonon activation energy (9.94 ± 0.6 meV) from the data plotted in Fig. 4(a).

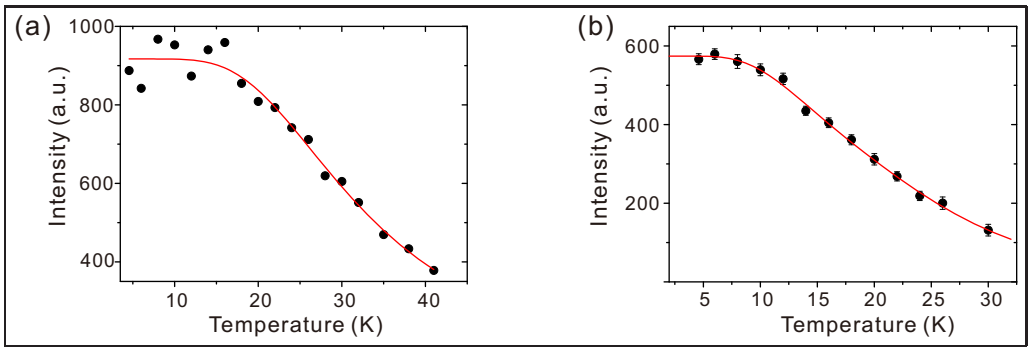

Fig. 4. (a) and (b) Integrated intensity as a function of temperature for SQE$_A$ and SQE$_B$. The decrease of the intensity at high temperature is observed. The change in the slope is around 20K and 10K , respectively. The red lines are fitted by equation (3).

To shed more light into the competing processes which yield the temperature induced luminescence quenching, we measure the temperature dependence of luminescence lifetimes from the red-shifted emitter A in the range 4 to 45K. The excitation beam is the 475nm blue line, up-converted from a near-infrared Ti: Sapphire laser (central wavelength 950nm, repetition rate 82MHz, 3ps pulse width) . The emitted photons are filtered by the monochromator and detected by a Silicon-based avalanche photo diode (APD). The time resolved PL is measured using a time correlated single photon counting (TCSPC) card with the time resolution 450 ps. The excitation power is fixed at 40 μW for different temperatures. The black curve in Figure 5(a) exemplarily shows the luminescence decay at 24K. We can see a very fast decay occurring within the time resolution scale and a much slower decay with a lifetime $T_2 \approx 3.65 \pm 0.30$ns. Interestingly, when the temperature raises to 41K, T_2 decreases to 1.39±0.06ns and the fast decay part vanishes. Similar to the model in discussed in equation 2, the temperature dependence of the emitter lifetime can be modeled with a three level system, assuming one ground state (the empty crystal) and two competing excited states that contribute to the emission process. We apply the model discussed in [23]

$$T_2^{-1} = \frac{\Gamma_{bright} + \Gamma_{dark}}{2} - \frac{\Gamma_{bright} - \Gamma_{dark}}{2} tanh \frac{\Delta E}{2k_B T} \tag{4}$$

Here, T_2^{-1} is the observed exciton radiation rate, Γ_{bright} and Γ_{dark} are the decay times of the two competing channels, corresponding to the lower and upper emission states. The energy

difference between the two emission states ΔE could thermalize the exciton states by absorbing and emitting phonons. Figure 5(b) shows the radiation rates as a function of temperature. The round black circles are measured data and the red solid line is the fit using the equation (4). The fitted line reveals Γ_{bright} =9.12ns^{-1}, Γ_{dark} =0.19 ns^{-1} and ΔE =(9.6±0.74)meV. The large difference between the extracted emission rates at low and high temperatures suggests, that a dark exciton significantly contributes to the decay process. The energy difference between states extracted from these lifetime measurements neatly matches the characteristic energy scale which we extracted as the activation energy of LO-phonons in our emitters and furthermore was extracted as the activation energy from the temperature induced intensity quenching. It is worth noting, that the dark exciton configuration has been identified as the lowest lying state of the free exciton in WSe_2, with an energy separation on the order of 30-40 meV to the bright state [**?**] The presence of confinement, localization and strain variations at the interface to the bulk crystal can change this number somewhat, and a value of ΔE =(9.6±0.74)meV is well within the expected range [26].

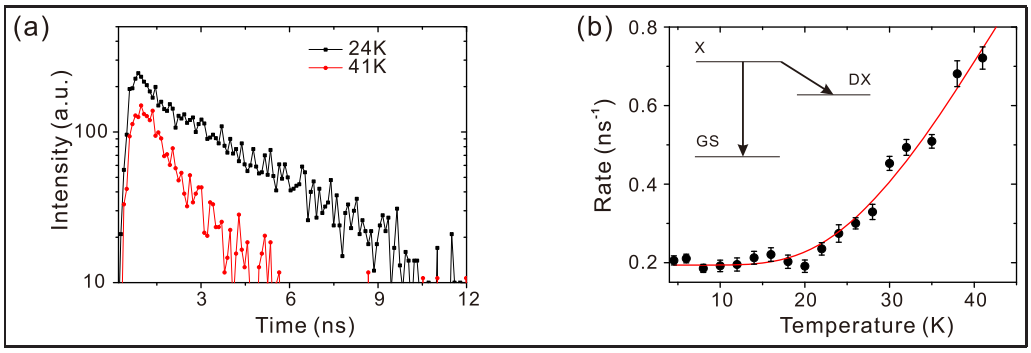

Fig. 5. (a) Time resolved PL of SQE_A. The black line decay is bi-exponential at 24K with the long decay time 3.65 ns. The red line is mono-exponential at 41K with the decay time 1.39ns. (b) Decay rates of SQE_A increase as a function of the temperature. The change of the slope is around 20K. The red line is fitted by equation (4).

4. Conclusion

In summary, we observed highly red-shift localized single emitter in a WSe_2 monolayer. The emission wavelength, which is in the transparent region of GaAs, outlines the possibility to integrate such emitters in GaAs based nano- or microphotonic architectures. The temperature dependent intensity decay and linewidth broadening reveal a dominant phonon influence on the single emitter. The assumption that a carrier transfer into a near lying dark state leads to the temperature induced luminescence quenching is backed by time resolved spectroscopy which sheds further light into the the basic energy structure of the localized emitters in monolayer semiconductors. The result was further supported by the recent discovered free dark exciton in monolayer WSe_2[26].

Funding Information

We acknowledge financial support by the State of Bavaria. Y.-M.H. acknowledges support from the Sino-German (CSC-DAAD) Postdoc Scholarship Program.

Acknowledgments

We thank Chaoyang Lu and Jianwei Pan for discussions and for providing the unique material. We furthermore thank Nils Lund, Oliver Iff and Isaak Kim for discussions and helpful assistance in characterizing the material.